Polymer Crystallization: Metastable Mesophases and Morphology

Eric B. Sirota*

Corporate Strategic Research, ExxonMobil Research and Engineering Company, Route 22 East, Annandale, New Jersey 08801

Received July 6, 2006; Revised Manuscript Received December 11, 2006

ABSTRACT: A path of polymer crystallization has recently been proposed by Strobl by which lamellae are first formed in a mesophase, which then convert to the crystal form with a nanoscale granular or blocklike structure. The crystallization temperature dependence of the lamellar thickness was argued to imply a transient mesophase. Here we argue that the granular structure of the lamellae is itself a fingerprint of the transient mesophase into which a lamella originally grows and its conversion to the higher-density stable form. The lower interfacial energy of the mesophases, which cause them to be favored as the initial growing phase, is directly connected to their lower density. The reduction in area at the mesophase-stable transition, being frustrated by the tethering of the stems to the amorphous region, results in the granular structure. We also discuss the effect of the relaxation of the stresses in the amorphous region and importance of hysteresis at the mesophase-to-crystal transition.

Introduction

The basic mechanisms of polymer crystallization have recently become the subject of renewed interest, study, and debate. Strobl et al. have shown clearly, through careful experimental methodology, that many semicrystalline polymers exhibit a granular substructure.[1−3] By relating the crystallization temperature, melting temperature, and crystalline lamellar thickness, they have shown that the thickness is related to the proximity of the crystallization temperature to a transition temperature located above the equilibrium melting temperature. [4−7] Their proposed mechanism and thermodynamic framework is that lamellar growth fronts are thin layers of a mesomorphic phase, which thicken until they reach a thickness where the stable crystal phase is favored. When the layers convert to the crystal phase, they can no longer thicken. The conversion occurs in a blockwise fashion, resulting in the observed granular structure; then a stabilization process occurs, which lowers the free energy of the newly formed crystallites so they do not return to the mesomorphic phase if the temperature is raised slightly. This route to crystallization was shown to apply to many cases in polymer crystallization.

Strobl's picture of crystallization is not yet generally accepted, particularly due to questions in the mechanism of the block formation and stabilization. However, we believe that the picture and thermodynamic framework are generally correct for many situations, and in this contribution, we explain the *direct connection* between the granular block structure and the transient mesomorphic phase. We also propose a specific stabilization mechanism derived from the block structure, but also show that such stabilization is not necessary to qualitatively explain the phenomena.

In short, it is the lateral density differences between mesophases and stable crystal phases, which give rise to the block structure when the lattice contracts, with the ends of crystalline stems kinetically tethered to positions in the amorphous melt set by the original mesophase packing density. Because of hysteresis, the conversion from the mesophase to the crystal phase will occur with some degree of supercooling ("superthickening") such that a slight temperature increase will not cause the crystal to revert to the mesophase, even without an additional stabilization of the crystal phase. Relaxation in the amorphous region relieving the stress on the crystal-phase packing density is a mechanism that would reduce the free energy of the crystal state, thus providing stabilization of the crystal phase against conversion back to the mesophase on further increase in temperature.

We believe that this will strengthen the argument for an important route of crystallization being mediated by transient mesophases and provide a clear connection to the granular block morphologies observed.

Background

It is now clear that many semicrystalline polymers exhibit a granular substructure.[4,6,8] This structure was directly observed by AFM. The broken crystal registry between these domains is manifest as a coherence length of the peak widths in wide-angle X-ray scattering ("in-plane") 200 or 110 reflections. These X-ray-derived sizes were shown to be consistent with the AFM-imaged domain sizes.

For an ordered phase to crystallize from the amorphous melt, a nucleation barrier resulting from the interfacial energy between that ordered phase and the melt must be overcome. This results in supercooling. As Ostwald's rule of stages implies, if the nucleation barrier for the stable phase to appear out of the melt is sufficiently high, another phase with a lower nucleation barrier, having a free energy intermediate between that of the stable phase and the melt, will be the one to form.[9] This could be, for example, the hexagonal phase in polyethylene.[10]

The role of transient metastable phases in the nucleation of polymer crystals has been a subject of increased recent interest.[11] Evidence that crystallization in such semicrystalline polymer systems is mediated by a transient metastable phase had been given by Keller, who argued in favor of its general role.[10,12] This was directly demonstrated for polyethylene oligomers (*n*-alkanes)[13,14] and an alkyl-cyclohexane.[15] These shorter molecules are relevant because Ungar had shown that the rotator phases in shorter alkanes and the hexagonal phase in polyethylene are the same entity on a qualitative continuum.[16] The crossover from the smaller supercoolings for homogeneous nucleation of the alkanes to the larger supercooling in the high-MW polymers begins at rather low MW, in the range of carbon number $n \sim 20$, suggesting a strong connection between alkane and polymer nucleation mechanisms.[17]

* E-mail: Eric.B.Sirota@ExxonMobil.com.

10.1021/ma0615147 CCC: $37.00
Published on Web 01/26/2007

A second process by which the metastable phase converts to the stable phase is rapid in some cases and slow in others. In alkanes, such variation of the rate of conversion was observed,[14] and the nucleation of the crystal phase from the rotator phases was also characterized.[18,19] By observing the lamellar thickness as a function of crystallization temperature and melting temperature for a variety of semicrystalline polymers, Strobl[2−5,7] gives very convincing evidence that the lamellar thickness is determined by the transition between a metastable mesophase and the stable crystal phase.

From nucleation theory, we know that the nucleation rate is a very strong function of interfacial energy. The interfacial energy between two phases is very much related to how different they are from one another. In the simplest approximation, one can characterize a phase by its density and only then consider more subtle structural details such as chain order and conformation. The hexagonal phase of polyethylene has many gauche bonds and a high degree of disorder, with an entropy closer to the liquid than the crystal.[16] While this hexagonal phase may have long-range positional order of the chain's average positions, it is not a phase of well-ordered chains where every atom has a specific place on a hexagonal lattice. It is rather entropically stabilized. This is *generally true* for most mesophases, which may be crystalline in that they have long-range positional order of the average molecule, but where there is also a high degree of disorder. The important point here is that mesophases in general, and the hexagonal phase of PE (and rotator phases of alkanes) in particular, have a lower lateral packing density than the fully ordered crystal phase. In the case of polyethylene, the 2D packing density is ∼13% lower.[20]

It is important to consider the relative rates of the appearance (nucleation and growth) of the metastable phase and the rate of conversion of the metastable phase to the stable crystalline form. When the latter is slower, it makes it easier to experimentally detect the metastable phase. In the *n*-alkanes, the rate of conversion from the metastable rotator phase to the stable orthorhombic phase was shown to increase with decreasing temperature.[14] However, the implications for what one would expect for the crystal morphology in the metastable and stable phases has not been discussed. Crystallizing out of the melt, especially with short alkanes, large single crystals may form. Let us suppose that, in general, a large single-crystal layer of the metastable mesophase forms. For the alkanes and polyethylene, we know that there is a significant difference in structure and in-plane density between the hexagonal (rotator) and the orthorhombic crystals. There is a decrease in the area/molecule of ∼13% in going from hexagonal to orthorhombic in PE (less for the alkanes) with an accompanying distortion of the lattice, shown in Figure 1a.[21] In short alkanes, such a transformation could occur with lateral molecular diffusion in the solid state, allowing a large single-crystal to be maintained. However this macroscopic reorganization would not be possible in a polymer where the *entangled cilia in the amorphous regions would impede the crystalline stems from rapidly moving laterally any significant distance*.

Thus we can understand the origin of the granular structure as follows, shown schematically in Figure 2: Initial nucleation and growth occurs by stem addition, but into the mesophase. Lamellar thickening occurs while the chains are in the more mobile mesophase. When the thickness grows large enough to allow conversion from the mesophase to the crystal, the *average density in the lamellae has been set by the mesophase, and the crystal breaks up into blocks.*

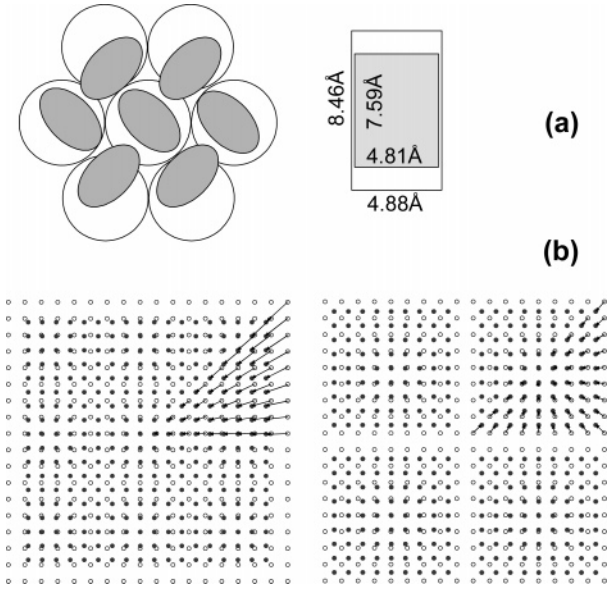

Figure 1. (a) Two-dimensional structures of the hexagonal (white) and orthorhombic herringbone crystal structure of polyethylene (shaded). The unit cells are shown in the figure. The 2D lattice expands 13%, while the bulk density increase is only ∼8.5% because the orthorhombic to hexagonal transition also involves the appearance of gauche bonds, which decrease the average distance along the *c*-axis from 2.53 to ∼2.45 Å .[21] Hexagonal is drawn here as an orthorhombic cell with lengths in the ratio of $\sqrt{3}$. (b) Schematic showing lattice contraction, on a square lattice. Displacement vectors are shown. When the contracted structure breaks into blocks, as shown on the right, the average displacement is much smaller.

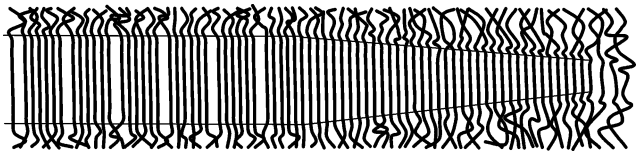

Figure 2. Schematic, after Strobl, showing the stem addition growth front, lamellar thickening in the M-phase, and conversion to the stable crystal where the granular structure develops.

In Figure 3a, we draw the T versus $1/n$ phase diagram with Gibbs−Thomson melting lines following Keller[10] and use Strobl's thermodynamic nomenclature. This shows the thermodynamic transition temperatures (equilibrium and metastable) between the amorphous-melt (a), mesophase (m), and crystal (c) phases as a function of crystalline lamellar thickness, n (in CH_2 monomer units).

In terms of the transition enthalpies (Δh) between the states, and the "end"- or "basal" surface-free energy per crystal stem (σ), the equilibrium transition temperatures are given by:

$$T_{cm} = T_{cm}^{\infty}\left[1 - \frac{2(\sigma_{ac} - \sigma_{am})}{n\Delta h_{mc}}\right] \qquad T_{ac} = T_{ac}^{\infty}\left[1 - \frac{2\sigma_{ac}}{n\Delta h_{ac}}\right]$$

$$T_{am} = T_{am}^{\infty}\left[1 - \frac{2\sigma_{am}}{n\Delta h_{am}}\right] \qquad T_{c'm} = T_{cm}^{\infty}\left[1 - \frac{2(\sigma_{ac'} - \sigma_{am})}{n\Delta h_{mc}}\right]$$

$$T_{ac'} = T_{ac}^{\infty}\left[1 - \frac{2\sigma_{ac'}}{n\Delta h_{ac}}\right] \tag{1}$$

As shown in Figure 3, the M-phase is stable with respect to the amorphous phase, after crossing to the left of T_{am}. Thickening moves to the left, where eventually the C-phase is stable when crossing T_{cm}.

Strobl considers a native crystal phase (cn ≡ c here), which is the structure into which the orthorhombic crystal initially

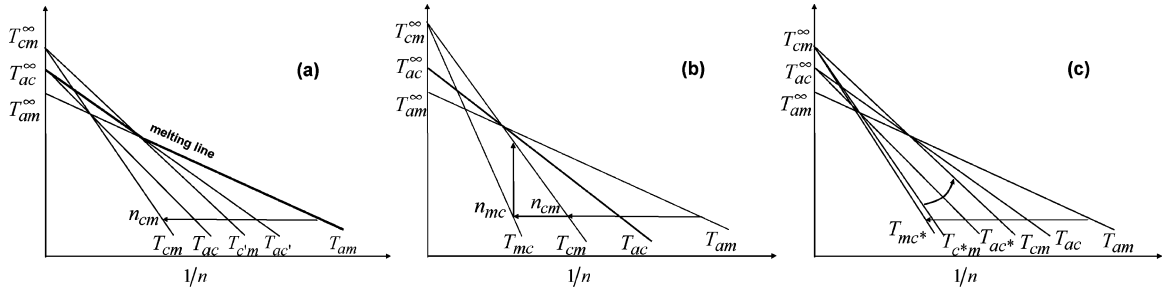

Figure 3. (a) Temperature−thickness phase diagram with stabilization. (b) Phase diagram with "superthickening" hysteresis. (c) Phase diagram with lateral relaxation and some hysteresis. Except for the T_{mc}, the T_{ij} represent equilibrium thickness-dependent transition temperatures between the two states; where a = amorphous, m = mesophase, c = crystal, and c′ & c* are stabilized or relaxed crystal structures as described in the text. T_{mc} represents the observed transition temperature and differs from T_{cm} due to hysteresis. T_{∞} are the infinite thickness values for these equilibrium transition temperatures.

forms, and a "stabilized" state (cs ≡ c′ here) into which it transforms over time. The principal difference between these, in Strobl's formulation, is that $\sigma_{ac'} < \sigma_{ac}$. After converting from M → C, Strobl postulates that C stabilizes into C′. Thus, as can be seen in Figure 3a, on raising temperature, the structure will not convert back to the M phase until the $T_{c'm}$ line is reached. If one crosses the $T_{c'm}$ line into the M-phase before melting, then "recrystallization" will occur, where the lamellae will again thicken. Strobl uses the thicknesses thus measured to determine the curve associated with the equilibrium transition between the "stabilized" crystal phase and the mesophase, $T_{c'm}$.

M → C Conversion and Superthickening. When the thickness exceeds n_{cm}, (moving to the left, crossing T_{cm} in Figure 3b), the crystal phase becomes more thermodynamically stable than the mesophase, and the M → C transition *may* occur. Here, Strobl assumes that the conversion actually occurs exactly on the T_{cm} line, so $n = n_{cm}$.

$$n_{cm} = \frac{2(\sigma_{ac} - \sigma_{am})}{\Delta h_{cm}(1 - T/T^{\infty}_{cm})}$$

However, the transition will not occur immediately when it is only infinitesimally thermodynamically favored. To the extent that the mesophase does not convert to the crystal phase instantaneously on reaching a thickness n_{cm}, the lamellae will continue to thicken. We then must consider both the process of spontaneous nucleation of C in the midst of the thicker part of the M-phase as well as the rate of propagation of the M → C transition into the mesomorphic region. We consider a few cases.

First, we ask what happens if the spontaneous nucleation of the M → C transition is very slow, so slow that the growth of the mesophase lamella is essentially already complete. In that case, the lamellae would thicken to be wedge-shaped-like in Figure 4a. This is not the dominant morphology reported by Strobl, but perhaps may occur in some polymer systems.

Another case depicted in Figure 4b is where the initial nucleation step of M → C takes place after a finite time, but while the lamellae is still growing. In such a case, the portion of the lamellae which was first to form may still have grown rather thick before the M → C transition suppressed thickening. In this limit, there may be a narrow, thicker wedge region that could potentially be detectable. Once the M → C transition has nucleated, the M → C front can follow the A → M stem-addition growth front, but can get *no closer than* the point where the thickness is $n = n_{cm}$. Figure 4b depicts this situation, where the transition occurs when $n = n_{cm}$.

The next question is whether the maximum front velocity of the M → C transition is faster or slower than the growth rate of the A → M front. If the M → C was slower, then a wedge

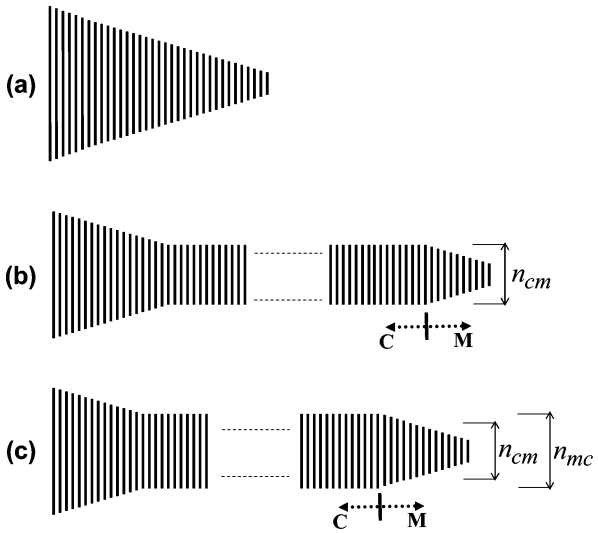

Figure 4. Schematics showing hypothetical thickness profiles based on nucleation and propagation of the M → C transition. (a) Wedge-shaped lamellae morphology that would be expected if the M → C conversion occurred very late. (b) Situation if M → C nucleation occurs with some delay but while the lamellae is still growing. After nucleation, the transition occurs behind the growth front when $n = n_{cm}$. (c) M → C transition does not occur at its thermodynamic stability point, but requires a finite driving force, so "superthickening" will occur and $n = n_{mc} > n_{cm}$.

shape (as Figure 4a) would result, but we do not believe this is the case. We suggest that the spontaneous nucleation of the M → C may be delayed, but because this transition does not involve macroscopic rearrangement, once nucleated, it could move through the crystal faster than the stem-addition A → M growth front, keeping up with it and resulting in a steady-state growth behavior. Such behavior is consistent with the dominant behavior described by Strobl, where the thickness is essentially constant for most of the lamellae.

Considering now steady-state stem-addition, thickening, and M → C conversion, we now want to know what the thickness of the lamellae will be when thickening is suppressed at the transition. One might associate this thickness with that at thermodynamic equilibrium between the mesophase and the crystal (n_{cm}), as we show in Figure 4b. However, n_{cm} is only the thickness at which the driving potential for the M → C transition is identically zero, becoming finite and increasing as $n > n_{cm}$. So under isothermal conditions, we might assume a constant lateral growth rate for the A → M stem-addition front. The lateral speed of propagation of the M → C transition will increase with $n - n_{cm}$. The essential point here is that the actual thickness at which the transition occurs (which we denote as n_{mc}) will be larger than n_{cm} and determined by the condition

that the speed of propagation of the M → C transition matches that of the A → M stem-addition growth front, giving the situation shown schematically in Figure 4c.

The existence of this hysteresis allows a simplification to the "necessary" elements of Strobl's framework. He assumed $n = n_{mc} = n_{cm}$ such that without a "stabilization" process (where the C-phase surface energy is reduced), the n_{cm} crystallites would undergo a transition back to the mesophase on slight elevation of the temperature. However, as we just explained, the finite propagation rates of the M → C transition results in $n > n_{cm}$, and so C will be stable with respect to a transition back to M upon a slight temperature increase. While this simplifies the framework, it also implies that the measured T_{mc} vs $1/n$ is not exactly the equilibrium curve, and the surface energy derived from the slope of that curve is not the true surface energy.

In Figure 3b, we show the phase diagram drawn with this "superthickening" hysteresis rather than stabilization. The T_{mc} line on Figure 3b is not a thermodynamic boundary. Its position below T_{cm} represents the kinetic delay. Because the *x*-axis is $1/n$, the shift must slow approaching the *y*-axis. Thus for $n \rightarrow \infty$, $T_{mc} \rightarrow T_{cm}$, with T_{mc} decreasing with a greater slope. Making a linear approximation, we thus write empirically $T_{mc} = T_{cm}^{\infty}[1 - (2\beta(\sigma_{ac} - \sigma_{am}))/n\Delta h_{mc}]$, where the empirical constant $\beta > 1$.

In Strobl's formulation, the surface energy of the melting line is associated with a stabilized crystal $\sigma_{ac'} < \sigma_{ac}$, and for sPP, he extracts from the slopes:[4]

$$\text{(from melting line) } \sigma_{ac'} = 7.5 \text{ (kJ/mol)}$$

$$\text{(crystallization line) } \sigma_{ac} - \sigma_{am} = 5.6$$

$$\text{(recrystallization line) } \sigma_{ac'} - \sigma_{am} = 4.1 \text{ thus } \sigma_{ac} = 9.0 \text{ and } \sigma_{am} = 3.4$$

Assuming that there is only "superthickening" and not "stabilization", we obtain:

$$\text{(from melting line) } \sigma_{ac} = 7.5$$

$$\text{(from recrystallization line) } \sigma_{ac} - \sigma_{am} = 4.1 \text{ thus } \sigma_{am} = 3.4$$

$$\text{(from crystallization line) } \beta(\sigma_{ac} - \sigma_{am}) = 5.8 \text{ thus } \beta = 1.4$$

While we argued above that a finite superthickening must be expected and that $T_{mc}(n)$ is not the equilibrium transition temperature, we do not know the magnitude of the hysteresis or whether it accounts fully for the experimental results. In fact, below we will show that a stabilization should indeed *also* occur.

Granular Structure

The above discussion involved lamellar thickening and the interfacial energies of the "end" surfaces of the lamellae. *However, the transition from the mesophase to the crystal phase also involves a non-negligible increase in the lateral packing density*.

In semicrystalline polymers, entanglements in the amorphous region, as well as chain folds and lamellar-spanning chains, will have the effect of limiting the allowable lateral displacement of the crystalline stems during the rapid solid-state transformation from the mesophase to the crystal form. (This is in contrast to short alkanes, where each stem is independent and lateral molecular diffusion in the solid-state could more freely occur.) Thus, over long distances (and short times), the stems are kinetically constrained to be close to the lateral position at which they grew in the mesophase, while the local packing now favors the more stable crystal phase with a higher lateral density. The constraints on the chain ends favoring the lateral density of the mesophase, competing with the density of the thermodynamically favored crystal structure, gives rise to a frustration that will cause the crystal to break up into domains. Here, the lateral density measured over long distance is the lower density of the mesophase, and the local packing has the structure and higher density of the (in the case of PE, orthorhombic) crystal. In fact, Strobl had noted that the average density of the lamella is only ~81% of the actual crystal density based on the local crystal structure.[7]

It is apparent (see Figure 1b) that the average displacement of molecules from their initial positions is minimized when the contraction occurs in smaller domains. When considering competing length scales, (or wavevectors in reciprocal space, q_1 and q_2), such frustration gives rise to a modulation with a wavevector $q_{mod} = q_1 - q_2$, in the limit of no elastic strain. In fact, Strobl noted[2] a potential similarity between these and the ripple phase of phospholipids that may arise from competition between the preferred packing densities of molecular heads and tails.[22] The crystalline structures are anisotropic, and there is not extensive detailed data on the anisotropy of the block sizes. However, taking an average of the area per molecule of $A_1 \sim 19.5$ Å^2 in the rotator phase and $A_2 \sim 18$ Å^2 in the crystal phase, we compute $\Delta q = 2\pi/\sqrt{A_1} - 2\pi/\sqrt{A_2}$ or a modulation period of ~108 Å, which is of the same order of what is observed. (There are some results on the anisotropy of the domain sizes, which suggest a shorter modulation period along the 200 direction, which is directionally consistent with this argument.)[8] This only gives a simple phenomenological estimate for the block size.

Microscopically and energetically, the domain size can be related to the competition between the energetic cost of a domain wall and the elastic-like energy associated with "stretching" a chain that is "tethered" (at least over the timescale of granular breakup) in the amorphous region. In this way, the thermodynamics strongly favor the crystalline close-packing, while the linkage to the amorphous region imposes a lower overall density. (In addition, an elastic response of the local lateral density of the orthorhombic crystalline region can also be taken into account so that actual local packing may be close to that of the ideal orthorhombic crystal, but perturbed due to the stress.) We are approximating here the situation where the stem-packing changes rapidly compared to the diffusive dissipative response of the amorphous melt structure such that it behaves elastically. The nature of these timescales and how they change with polymer MW is an important question for future study.

The energetics associated with the domain formation will actually affect the thermodynamics of the phase transitions and therefore modify the expressions given in eq 1 above. Here we describe a highly simplified elastic model. The finite thickness of the crystal layers (n) has already been included in the free-energy used by Strobl, which accounts for the end-surface energy (σ) of both the crystal and meso-phases. We now need to account for the finite lateral size of the domains. Such a term is relevant only in the C-phase because a continuous layer is assumed to grow in the M-phase. We define ϵ as the edge-surface energy of a C-phase domain (energy per unit area), and ν = volume per monomer unit. The free energy per monomer due to the edge surface, for domains of diameter D is:

$$g_{edge} = 4\epsilon\nu/D$$

We model an effective elastic energy g_{end_strain} associated with the crystal stems having a spacing a_c being "anchored" into the

amorphous region with spacing a_m (set by the mesophase spacing). This will increase with the size of the domain (as depicted in Figure 1). We make a simple assumption that the energy cost per stem is $\lambda\delta$,[2] where δ is the lateral distance of the stem from its "anchoring" point. (We approximate that this energy cost does not decrease with the length of the stem, and we treat a crystal without 2D anisotropy.) Averaging over a circular domain, we obtain

$$g_{\text{end\_strain}} = \lambda D^2(a - a_m)^2/8a^2n$$

We could include another elastic term to allow strain of the crystal structure away from a_c, but for the present purposes, we assume that $a = a_c$.

Minimizing the free energy $g_D = g_{\text{edge}} + g_{\text{c\_strain}}$ in D, we obtain:

$$D^{*3} = \frac{16n\epsilon\nu}{\lambda(1 - a_m/a_c)^2} \text{ with } g_D^* = 6\epsilon\nu/D^*$$

Thus the selected domain size, D^*, will increase with the thickness of the layer and grow with smaller packing mismatch. The main point is that D^* will increase with n, and that D^* and g_D^* are determined from the competition of the edge surface energy and strain.

The Gibbs free energy difference between the various phases are then:

$$\begin{aligned} g_c - g_a &= \Delta s_{ac}(T - T_{ac}^\infty) + 2\sigma_{ac}/n + g_D^* \\ g_m - g_a &= \Delta s_{am}(T - T_{ac}^\infty) + 2\sigma_{am}/n \\ g_c - g_m &= \Delta s_{cm}(T - T_{cm}^\infty) + 2(\sigma_{ac} - \sigma_{am})/n + g_D^* \end{aligned} \quad (2)$$

Setting these to 0 gives the phase boundaries, where we assume that the domain size, D, is chosen to minimize the free energy at the M → C transition.

$$T_{c^*m} = T_{cm}^\infty - \frac{2(\sigma_{ac} - \sigma_{am})}{n\Delta s_{mc}} - \frac{6\nu\epsilon}{D^*\Delta s_{mc}}$$

$$T_{ac^*} = T_{ac}^\infty - \frac{2\sigma_{ac}}{n\Delta s_{ac}} - \frac{6\nu\epsilon}{D^*\Delta s_{ac}} \qquad T_{am} = T_{am}^\infty - \frac{2\sigma_{am}}{n\Delta s_{am}}$$

We see that the edge surface energy term's contribution goes as $1/D$. As $n \to \infty$, D will also diverge. (Above, we calculated that D scales as $n^{1/3}$ rather than the linear dependence suggested by Strobl's data,[1] but here we employed an admittedly oversimplified elastic model.) The basic trends are important here, and in the schematics of Figure 3c, we draw the phase boundaries as linear in $1/n$.

In the framework described here, the spontaneous nucleation of the M → C transition occurs once in the lamellae and then propagates a finite distance behind the $n = n_{mc}$ thickening front. Thus each of the blocks is *not* the result of independent M → C primary nucleation event. In Figure 5, we show schematically how the M → C transition might propagate. As the M → C front passes, the molecules locally pack closer, the frustration occurs, and the structure breaks into the granular structure behind the transition front.

Stabilization

A specific stabilization process now naturally derives from this picture. After the crystallization and block formation (shown in Figure 5) is complete, there is still stress caused by the mismatch of the crystal spacing and tethered amorphous chains.

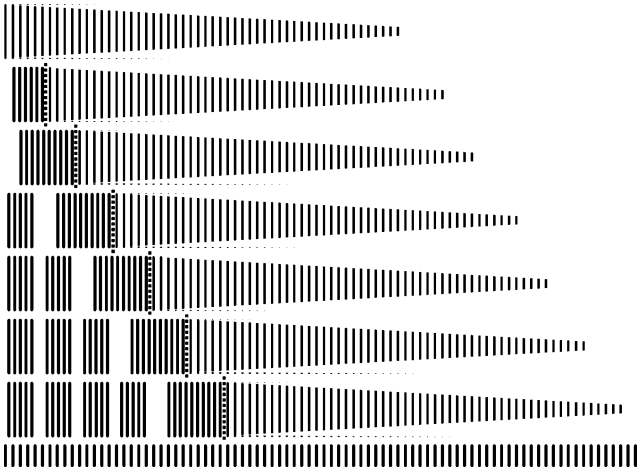

Figure 5. Progression of the A → M growth front and the M → C conversion front, leaving blocks formed in its wake. On the bottom, the original M-phase periodicity is shown. The initial nucleation of C is not shown. The thinner lines represent molecules in the M-phase, and the thicker lines are those packed in the C-structure. The transition front is noted with the thick dashed line.

During the relatively rapid transformation from M → C, the stems behaved as though they were anchored to the positions in which the mesophase grew. However, this tethering is to the amorphous melt and over time; after the crystal domains have formed, chain relaxation, slow on the timescale of the initial crystallization, will reduce the stress.

Two possible paths of relaxation are shown schematically in Figure 6: (a) With the stem packing that formed the crystalline block structure held fixed, the amorphous region could relax to accommodate that stem packing. This would lower the free energy of the existing structure. In terms of the elastic model above, this would reduce g_D from $g_D^* = 6\epsilon\nu/D^*$ to $g_D = 4\epsilon\nu/D^*$. Thus the elastic term would disappear, but the edge-surface contribution would be unchanged. This mode of relaxation in the amorphous region would be driven by the stresses on the amorphous chains being connected to the crystal. When such relaxation occurs, it will *further stabilize* the block structure, making it harder for the stems to subsequently diffuse and merge together, as described below. (b) Depending on the relative rates of diffusion and chain motion, it is also possible for the crystalline domains to coarsen or anneal, increasing D from D^*, with the amorphous region simultaneously rearranging to accommodate that. This would lower the free energy more that the previous case because $g_D = 4\epsilon\nu/D$ and $D > D^*$. Microscopically, one should consider this as a random diffusion, eventually driving the system to a lower energy state, rather than the previous case, where the relaxation is directed by a particular stress. This situation might be more likely to occur if temperature is raised and diffusion is faster.

In both cases, the free energy of the crystal phase will decrease relative to that of the mesophase. Thus the equilibrium phase boundary for C to convert back to M (i.e., T_{cm}) will be shifted up, providing stabilization for the C phase. This is shown in Figure 3c, where the curved arrow depicts the direction of relaxation, with the T_{cm} curve being the limit of the diffusive relaxation to continuous lamella with $D \to \infty$. We see that this is the same type of phase diagram as drawn by Strobl, with the boundaries having slightly different meaning. Because the effect of the stress term appears at the crystal−amorphous interface, although laterally inhomogeneous from a microscopic point of view (see Figure 1), it can be lumped into an effective "σ_{ac}", consistent with relaxation of $\sigma_{ac} \to \sigma_{ac'}$.

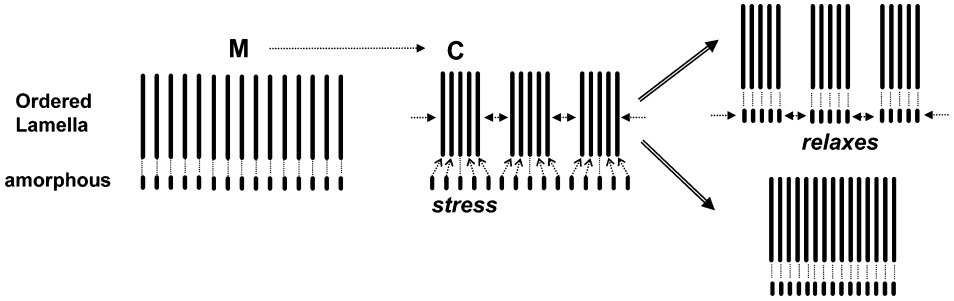

Figure 6. Schematic showing the stress and relaxation of the lateral density of the ordered lamella and amorphous region. (a) Showing relaxation driven by the stress. (b) Diffusion-driven relaxation minimizing the free energy.

Conclusions

We have shown how the block structure would result directly from the initial growth of a low-density ordered mesophase. Stabilization would naturally occur due to stress relaxation, although it will partly be an artifact of "superthickening".

One question raised by this proposition surrounds the relative relaxation rates in the entangled melt compared to the rate of already straight parallel chains adjusting themselves from a less-ordered packing to the more ordered one. In the case where the crystals are just short alkanes, there is no molecular connection to the melt region and there is thus no "tethering". For longer chains, those which only become semicrystalline with a finite lamellar thickness (shorter than the molecular length), it begins to be possible to have such a connection to the melt. Once the chains become long enough to be entangled, the relaxation of the chains in the melt can become extremely slow.

Transient anchoring of the crystalline stems to the melt/amorphous region will occur when this timescale is slow compared to the time to undergo the, e.g., rotator to orthorhombic transition. One expects this rearrangement to occur extremely rapidly once nucleated. The relevant time here being not the time it takes to thicken enough to want to undergo the transition, or even the (average) time to nucleate such a transition, but rather the rate of propagation once nucleated. This transition does not involve any macroscopic rearrangement, reptation, or motion, just local rotation and gauche−trans conformational changes of already nominally elongated and parallel stems. Thus, this could be expected to occur much faster than pulling chains out of the melt.

This suggests experiments looking at the granular structure as a function of polymer MW as it decreases below entanglement where tethering would be lost; these questions also show the need for molecular dynamics modeling to look at the translational diffusion in the melt compared to gauche−trans intramolecular motion in the ordered states. This would allow a more quantitative description of the "tethering", which could have both elastic and dissipative components.

Other questions are left open, such as the relative magnitude of the kinetically limited superthickening hysteresis as compared to the stress relaxation at the C → A interface, which would stabilize the C phase. This suggests time-dependent experiments that could differentiate these phenomena. Other questions for investigation include: (1) the relation between the anisotropy in the orthorhombic crystals and anisotropy, if any, in the block structure, and (2) the change in the block size with time, which would shed light on the stabilization mechanisms. We have not yet addressed the question of the breaking of hexagonal symmetry going to the orthorhombic crystal phase and effect of the block domain boundaries on choosing the crystallographic direction of the orthorhombic structure. Another interesting question is whether there is any superstructure ordering of the blocks and whether they form a two-dimensional structure, as do other modulations due to packing frustration.[23] Experiments specifically looking at the strain in the lamella (110 and 200 peak positions) would shed light on the stresses in the crystals arising from the amorphous layers. The elastic model given here for the amorphous−crystal interface is highly oversimplified, and a more detailed treatment is clearly necessary.

We suggest that the granular substructure observed in polymer crystals is a fingerprint of the transition from the transient intermediate state from which the crystal derived. Combined with different crystallization and Gibbs−Thomson melting lines and observed transient metastable phases in similar systems, this further strengthens the case for a "major route"[2] to crystallization being through a transient metastable mesophase.

Acknowledgment. I thank Scott Milner for a critical reading of the manuscript.

References and Notes

(1) Hippler, T.; Jiamg, S.; Strobl, G. *Macromolecules* **2005**, *38*, 9396.
(2) Strobl, G. *Eur. Phys. J. E* **2000**, *3*, 165.
(3) Hugel, T.; Strobl, G.; Thomann, R. *Acta Polym.* **1999**, *50*, 214.
(4) Strobl, G. *Prog. Polym. Sci.* **2006**, *31*, 398.
(5) Strobl, G. *Eur. Phys. J.* **2005**, *18*, 295.
(6) Heck, B.; Hugel, T.; Iijima, M.; Strobl, G. *Polymer* **2000**, *41*, 8839.
(7) Heck, B.; Hugel, T.; Iijima, M.; Sadiku, E.; Strobl, G. *New J. Phys.* **1999**, *1*, 11.
(8) Goderis, B.; Reynaers, H.; Scharrenberg, H.; Mathot, V.; Koch, M. *Macromolecules* **2001**, *34*, 1779.
(9) Ostwald, W. *Z. Phys. Chem.* **1897**, *22*, 286.
(10) Keller, A.; Hikosaka, M.; Rastogi, S.; Toda, A.; Barham, P. J.; Goldbeck-Wood, G. *J. Mater. Sci.* **1994**, *29*, 2579.
(11) Keller, A.; Cheng, S. Z. D. *Polymer* **1998**, *39*, 4461.
(12) Rastogi, S.; Hikosaka, M.; Kawabata, H.; Keller, A. *Macromolecules* **1991**, *24*, 6384.
(13) Sirota, E. B.; Herhold, A. B. *Science* **1999**, *283*, 529.
(14) Sirota, E. B.; Herhold, A. B. *Polymer* **2000**, *41*, 8781.
(15) Sirota, E. B.; Herhold, A. B.; Varma-Nair, M. *J. Chem. Phys.* **2000**, *113*, 8225.
(16) Ungar, G. *Macromolecules* **1986**, *19*, 1317.
(17) Kraack, H.; Deutsch, M.; Sirota, E. B. *Macromolecules* **2000**, *33*, 6174.
(18) Herhold, A. B.; King, H. E.; Sirota, E. B. *J. Chem. Phys.* **2002**, *116*, 9036.
(19) Nozaki, K.; Hikosaka, M. *J. Mater. Sci.* **2000**, *35*, 1239.
(20) Bassett, D. C. *Polymer* **1976**, *17*, 460.
(21) Bassett, D. C.; Block, S.; Piermarini, G. J. *J. Appl. Phys.* **1974**, *45*, 4146.
(22) Carlson, J. M.; Sethna, J. P. *Phys. Rev. A* **1987**, *36*, 3359.
(23) Sirota, E. B.; Pershan, P. S.; Deutsch, M. *Phy. Rev. A* **1987**, *36*, 2902.

MA0615147